DATA PROCESSING FOR A LANDMINE DETECTION DEDICATED GPR

J. Groenenboom
Section of Applied Geophysics,
Faculty of Applied Geoscience, Delft University of Technology,
Mijnbouwstraat 120, 2628 RX Delft, The Netherlands
J.Groenenboom@TA.TUDelft.nl

A.G.Yarovoy
International Research Centre for Telecommunications-transmission and Radar,
Faculty of Information Technology and Systems, Delft University of Technology,
Mekelweg 4, 2628 CD Delft, The Netherlands
A.Yarovoy@ITS.TUDelft.nl

ABSTRACT

The requirements on GPR technology for the application of humanitarian landmine detection are severe; 99.6% probability of detection and low false alarm rate. Trying to meet these challenging requirements, an impulse radar system has been designed specifically for the application of landmine detection. The radar system contains a dielectric filled TEM horn transmitting antenna and a small loop receiver antenna below the transmitting antenna.
With this radar system three-dimensional measurements have been carried out over a test site containing surface-laid and shallowly buried landmines. The test site contains antitank and antipersonnel mines of metal and plastic.
In order to show the performance of the new radar system we have to produce images of the subsurface. The imaging algorithms must then be tuned to the specific acquisition parameters. More specific, the refraction of the waves at the surface and the acquisition geometry of the transmitting and receiving antenna influence the arrivaltime of backscattered energy related to subsurface objects. Since imaging algorithms are based on coherent stacking over this energy we must take into account these factors.
We produce clear images of landmines and other subsurface objects using adapted imaging algorithms on the data obtained with the new radar system.

Key words: video impulse system, landmine detection, three-dimensional processing and imaging.

INTRODUCTION

Ground penetrating radar has proven to be a successful tool for subsurface characterization. However, for the application of landmine detection using GPR the current state of technology needs improvement. This is not only true for hardware, but for signal processing algorithms as well. To optimize the measurement from a hardware point of view, a new impulse radar has been built at the International Research Centre for Telecommunications-transmission and Radar (IRCTR). Details about the hardware characteristics and properties of this radar systems are presented in an accompanying paper (Yarovoy, van Genderen and Ligthart, 2000). For the application of landmine detection we should acquire ultra-wideband, high dynamic range data with antennas elevated above the ground. The generator spectrum covers a wide frequency band from 500 MHz until 2 GHz on 3 dB level. The 12-bit A/D converter provides 66 dB linear dynamic range. According to simulations this dynamic range should be sufficient to detect both antitank and antipersonnel mines in typical ground conditions. For the transmitting antenna an ultra-wideband dielectric filled TEM horn (DTEM) has been designed (Yarovoy, Schukin and Ligthart, 2000). For the receiving antenna a small loop is placed below the transmitting antenna. The developed antenna system possesses very small ringing and has been patented (de Jongh et. al., 1994).
For the purpose of three-dimensional subsurface imaging traces (A-scans) have to be acquired over a two-dimensional area, with fine spatial sampling (Groenenboom and Slob, 2000). Related to practical difficulties during acquisition, data are often not acquired on a regular spatial grid.
Due to the specific antenna geometry, the elevated measurements and the two-dimensional irregularly positioned data, we have to modify standard processing and imaging algorithms. Here, we show how to implement these factors without severely compromising CPU-time.

DATA ACQUISITION

The data have been acquired over a sandbox of 8 by 2.5 meter using a non-metallic mechanical scanner. Details about the scanner and the test site are presented in Jong,

Lensen and Janssen (1999). Along a line the mechanical scanner was moving with a more or less constant velocity and traces were continuously recorded. Roughly 400 traces were measured at a line with an average inline step of 2.1 cm. Small variations of this inline step occur because of non-constant movement of the scanner. 50 lines were recorded with a constant crossline step of 5 cm in alternating directions. This data acquisition resulted in low crossline continuity. In Figure 1 we show the inline positions for all traces. The alternating sequence is caused by the fact that acquisition along lines was carried out in alternating forward and backward directions.

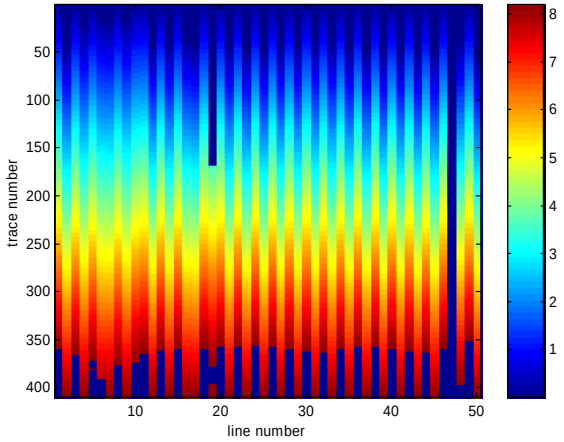

Figure 1: The inline position in meters as a function of the line number and trace number.

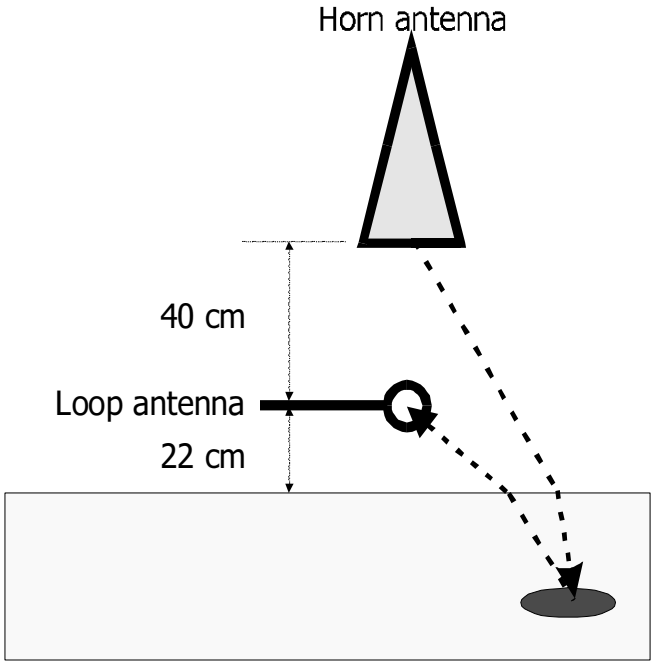

Figure 2: Geometry of the transmitting dielectric filled TEM-horn and the small loop positioned below the transmitting antenna.

The data have been measured with the loop antenna elevated 22 cm above the ground. The loop receiver has a vertical offset of 40 cm with respect to the transmitting transducer, see Figure 2.
Detailed information on the exact type and location of the landmines has not been provided. To test the performance of various technologies different types of landmines have been used, metallic and plastic (minimum metal) buried at different depth levels (Jong, Lensen and Janssen, 1999).

PREPROCESSING

An example of a line of raw data is shown in Figure 3.

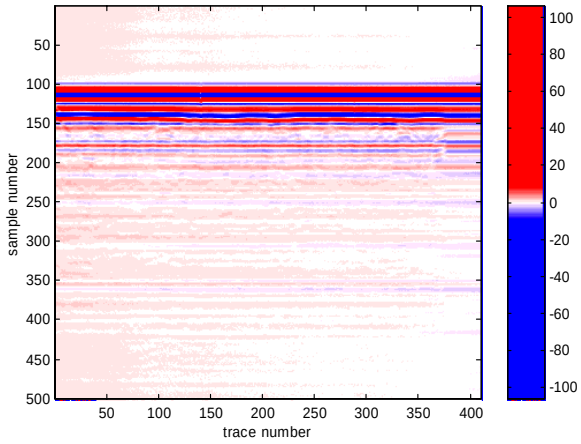

Figure 3: Plot of the raw data measured on a line. We mainly observe the strong direct wave and the surface reflection.

Before these data can be used in an imaging algorithm several preprocessing steps are carried out. These preprocessing steps include:

- Removal of the DC offset and DC offset drift. Due to problems during acquisition some traces were contaminated with a DC offset and sometimes a DC offset drift. We removed this noise by fitting a second order polynomial through the data and subtracting this polynomial from the data.
- Removal of traces with duplicates in position. Since the measurements were continued when the scanner stopped moving at the end of the lane, we deleted the duplicate traces in order to avoid weighting these data too strong.
- Alignment of time zero for all traces. Changes were observed in the arrivaltime of the direct wave, especially comparing different lines. We accomplished time equalization by aligning the first zero crossing of the direct wave.
- Subtraction of the direct wave. The direct wave was estimated by measuring the response of the radar in

laboratory conditions without backscattering from the surface or other scatterers. After aligning the zero crossing of this direct wave with the data we can subtract the direct wave from each trace.

- Filtering out the response of the strong surface reflection, and other strong horizontal events. For this purpose we apply two-dimensional moving average subtraction. Moving average subtraction is much better than global average subtraction because of topographic variations of the surface resulting in mainly time variations of the surface reflection. The moving average is estimated for each trace by stacking all adjacent traces within a certain circle and dividing by the number of traces. This moving average is subtracted from that particular trace, see Figure 4. It appears that two-dimensional moving average subtraction is much more stable than moving average removal along a line. In the latter case, strong backscattered energy is smeared out along the averaging window with opposite sign.

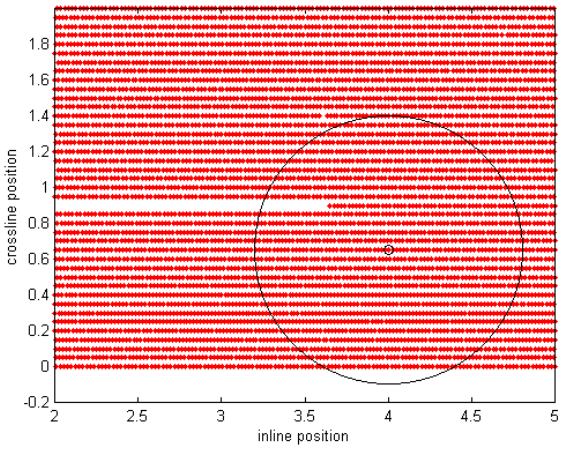

Figure 4: Determination of the moving average by selecting all traces within a circle and averaging for an irregularly positioned data set.

The data after preprocessing have a much better signal to noise ratio and are better fitted for the three-dimensional imaging algorithm, see Figure 5.

IMAGING

From our preprocessed data we can get a first indication of possible locations of objects, because of the presence of diffraction hyperbolas. However, to get better detectability and a more accurate indication of the position and size of objects, we want to apply an imaging algorithm. All imaging or migration algorithms are based on some kind of stacking of coherent energy based on back propagation.

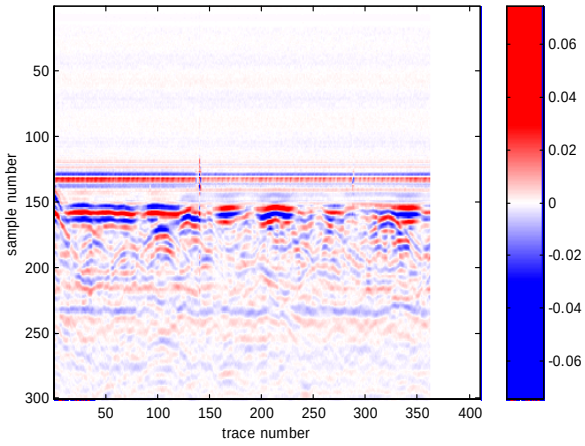

Figure 5: Same data as in Figure 3 after preprocessing**.**

For imaging, we use a diffraction stack in the spatial and time domain. Principally, this imaging is based on an estimation of an image value at a certain position by stacking the data associated with the appropriate arrivaltime for that specific location, i.e.

$$I(\mathbf{x}) = \sum_i d_i(t - T(\mathbf{x}, \mathbf{x}_i^S; \mathbf{x}_i^R)),$$

with image I, data d for all traces i, at the arrivaltime T of the wave for transmitting antenna position $\mathbf{x}_i^S$, image position $\mathbf{x}$, and receiver position $\mathbf{x}_i^R$.

We have chosen for this particular space/time domain technique because of its flexibility to handle irregularly positioned data. Since no spatial transformations are carried out such as in kf-migration (Stolt, 1978) we do not need to carry out regularization of the data in the spatial dimension. The specific irregular positions can cause artifacts in the image. However, it appears that no strong acquisition footprint is observed in the image, probably because no large gaps occur between traces. In addition, we can correct for the refraction at the surface by taking Snells law into account. This means that for every image position we have to calculate the traveltime from the elevated transmitting antenna to the image point and the traveltime from image point to elevated loop antenna, both by ray tracing through the air/soil interface. The correct ray is found using a root finding algorithm based on a bisection procedure combined with linear or quadratic inverse interpolation. In principle, the correct ray can also be found by solving a fourth order polynomial equation but the numerical root finding appears to be fast and accurate. The biggest price in performance is paid by the fact that we have irregularly positioned data. For regularly positioned data, traveltime templates can be calculated and used for every image point at the same depth level. For irregular data this regularity can not be exploited.

Since landmines can also be laid on the surface we want to image above the air-soil interface as well. In that case, we omit the correction for the refraction at the air-soil interface and trace the rays simply through the homogeneous air. In Figure 6 we show a selection of data containing a strong diffractor, combined with the traveltime curves for 20 depth levels, starting at 10 cm elevation and going deeper with a step of 2 cm. The strong diffractor present in this particular data is found at an elevation of approximately 5 cm. By stacking along the traveltime curve we obtain focusing of the image.

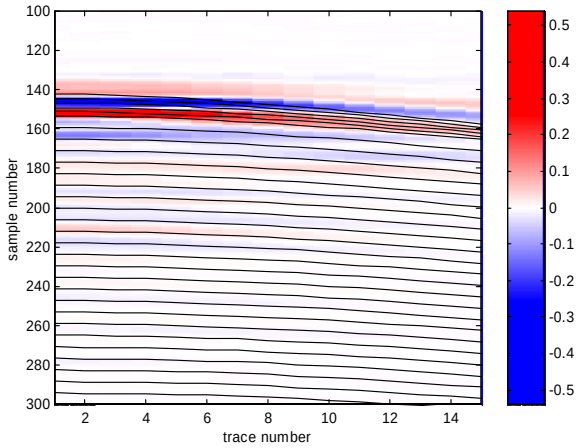

Figure 6: Subset of the data combined with the arrivaltime curves for a set of 20 depth levels.

EXPERIMENTAL RESULTS

We have produced image results over the whole area at a regular grid with inline and crossline spacing of 2 cm and from 10 cm above the air/solid interface until 50 cm below the air/soil interface, also with a step of 2 cm. For the imaging we use a relative permittivity of 7 for the sandy soil. In Figure 7 we show a subsection of the area imaged at 2 cm elevation. In this case we clearly see at least three large objects with an estimated size of roughly 30 cm. The depth, size and circular shape correspond to surface laid antitank landmines. In another section, see Figure 8, at the same 2 cm elevation we observe four significantly smaller circular objects with a size in the order of 10 cm. These four objects could be related to antipersonnel landmines, although at this point we can not make a definite statement whether or not these objects are false alarms.

As a last example, see Figure 9, we show a small section at a depth level of 30 cm below the surface. In this case we detect at least three objects ranging in size from 10 to 20 cm. The different strengths of the objects might also be related to whether these objects are metal landmines, plastic landmines or false alarms. The estimated depth of the objects is sensitive to the permittivity that is chosen in the imaging algorithm.

At several depth levels we detected a number of objects, differing in size and strength. Some, probably metal objects caused ringing in the signal, which also resulted in ringing of the object at several depth levels in the image domain.

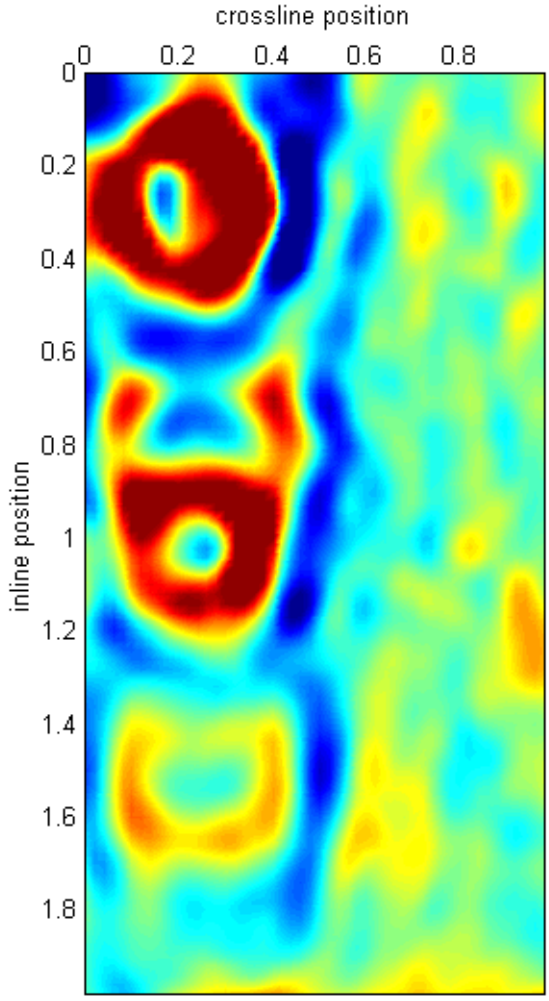

Figure 7: Subset of the image results, plan view at an elevation of 2 cm. We clearly observe three large objects

CONCLUSIONS

We observe that it is much easier to get an overview of possible locations of landmines within the area by using the plan view images, compared to cross-section plots of the preprocessed data, as in Figure 5. Because of the irregular positioning of the traces it is much harder to observe continuity of diffractors in the crossline direction. Applying moving average subtraction and diffraction stack algorithms in three dimensions appears to give much better results than using their two-dimensional equivalents, i.e. processing lines separately. The imaging results show that the newly developed radar can detect and image various objects of different sizes at different depth levels with high resolution.

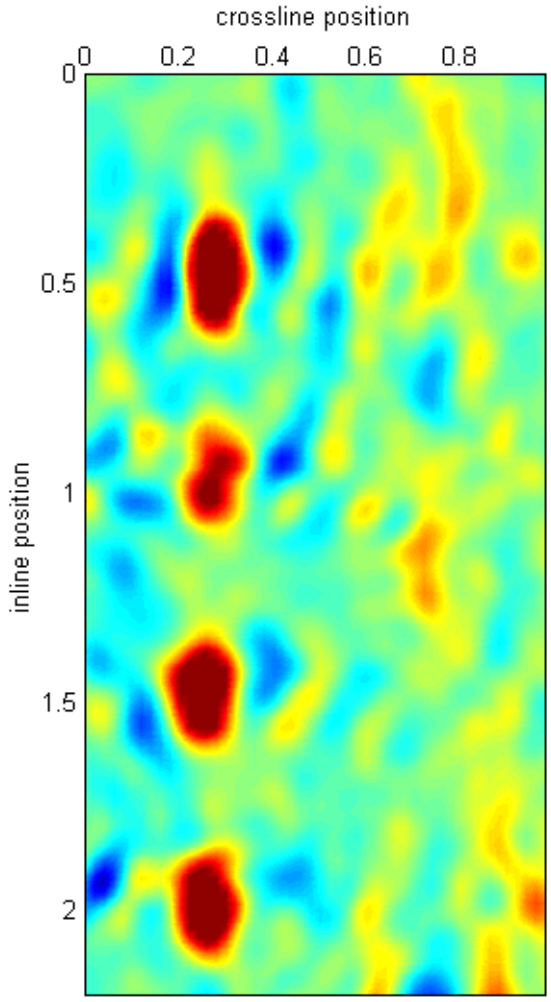

Figure 8: Plan view image results at an elevation of 2 cm, showing at least four clear objects, probably related to antipersonnel landmines

ACKNOWLEDGMENTS

This research is supported by the Technology Foundation STW, applied science division of NWO.

REFERENCES

Groenenboom J. and Slob E., 2000. Sparse data acquisition and its influence on imaging. *Proceedings on Ground Penetrating Radar Conference*, Gold Coast, Australia, 23-26 May 2000.

Jong, W. de, Lensen H.A. and Janssen Y.H., 1999, Sophisticated test facility to detect land mines, *Detection and Remediation Technologies for Mines and Minelike Targets IV, SPIE Proceedings*, Vol 3710, pp.1409-1418.

Jongh, R.V. de, Yarovoy A.G., Schukin A.D., Ligthart L.P., Morow I.L., *Penetrating air/medium interface microwave radar*, Patent 43107-NL, 24.11.1999.

Stolt, R. H., Migration by Fourier transform, 1978, *Geophysics*, Vol 43, pp. 23-48.

Yarovoy, A.G., van Genderen, P. and Ligthart, L.P. 2000 Ground penetrating impulse radar for landmine detection. *Proceedings on Ground Penetrating Radar Conference*, Gold Coast, Australia, 23-26 May 2000.

Yarovoy, A.G., Schukin A.D. and Ligthart L.P., 2000. Development of Dielectric Filled TEM-Horn. *Proceedings on Millennium Conference on Antennas & Propagation*, Davos, Switzerland, 9-14 April 2000.

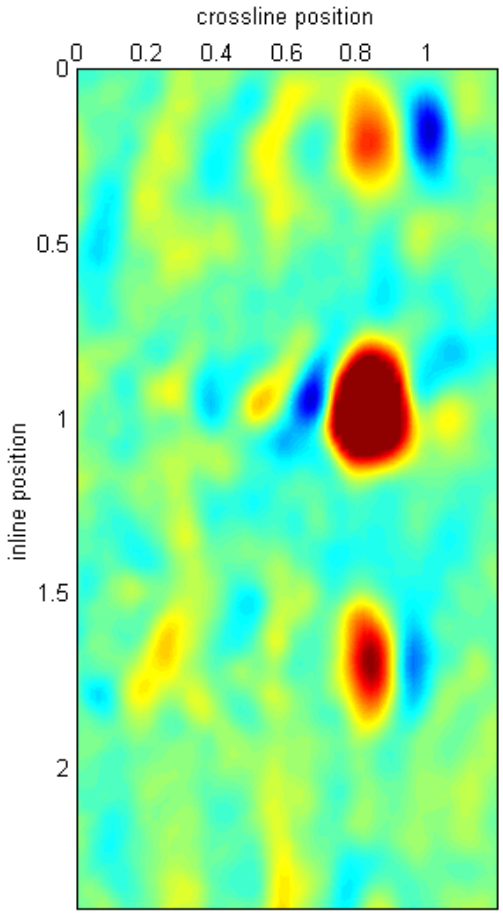

Figure 9: Plan view image results at a depth level of 30 cm showing at least three objects.